



## EXPERIMENTAL STUDY ON CARBON FIBER-REINFORCED SQUARE SEISMIC ISOLATORS

H.Toopchi-Nezhad<sup>1</sup>, M. Tait<sup>2</sup> and R.G. Drysdale<sup>3</sup>

### ABSTRACT

Steel reinforced elastomeric isolators (SREIs) have been used in many countries over the past three decades as an effective seismic isolation device. However, application of these devices, which are usually heavy and high-priced, is often limited to large and expensive structures. A reduction in the cost and weight of elastomeric isolators would permit a significant increase in their application to many residential and commercial buildings. Fiber-reinforced elastomeric isolators (FREIs) are a new type of laminated rubber bearings that utilize fiber (such as carbon fiber) as the reinforcement material instead of steel. FREIs have several advantages over traditional SREIs including: superior damping properties, lower manufacturing cost, light-weight, and the possibility of being produced in long rectangular strips with individual isolators cut to the required size. This paper presents a brief literature review on FREIs, and reports on an experimental study conducted on carbon-FREIs constructed at McMaster University, from which the mechanical properties of the bearings, including effective vertical and horizontal stiffnesses as well as damping ratios are evaluated. As a special application, the bearings were not bonded to the test platens. For bearings having suitable aspect ratio values, this particular type of application resulted in a stable rollover deformation, which reduced the horizontal stiffness and increased the efficiency of the bearing as a seismic isolator device. Test results suggest that for many high seismic risk regions in Canada, the application considered in this study for the base isolation of ordinary low-rise buildings is viable.

### Introduction

Steel-Reinforced Elastomeric Isolator (SREI) bearings are the most common type of isolator in use. SREIs are large, heavy and expensive; their application as a superior earthquake-resistant strategy is primarily justified for large and expensive buildings. Nevertheless, this justification cannot be easily extended to ordinary housing and commercial buildings. The heavy weight is due to the reinforcing steel plates. The high cost is primary due to the highly labor-intensive manufacturing tasks, and also the vulcanization process which occurs under high pressure and temperature (Kelly 2002). However, potential cost savings exist if the steel plates are replaced with other materials having approximately the same order of elastic stiffness as steel, so that the manufacturing process of the isolator becomes easier and less labor-intensive.

<sup>1</sup> PhD Candidate, Dept of Civil Engineering, McMaster University, Hamilton, ON, L8S 4L7, toopchi@gmail.com

<sup>2</sup> Assistant Professor, Dept of Civil Engineering, McMaster University, taitm@mcmaster.ca

<sup>3</sup> Professor Emeritus, Dept. of Civil Engineering, McMaster University, drysdale@mcmaster.ca

Fiber-Reinforced Elastomeric Isolators (FREIs) are a relatively new type of laminated bearing which utilize fibers as the reinforcing material instead of steel. Initial studies (Kelly 1999, 2002) indicated it is possible to achieve adequate vertical and horizontal stiffness in FREIs. Furthermore, FREIs have a number of advantages over SREIs including superior energy dissipation capability, potentially low manufacturing cost, light-weight, and the possibility of being produced in long rectangular strips and modified to the required size in the field.

The use of seismic isolation in new ordinary low-rise buildings cannot be extended unless an alternative strategy is adopted. Clearly, an alternative seismic isolation strategy should employ cost effective isolators in a simple application. Handmade square carbon FREIs, as an example of alternative isolators were studied in this research program. To reduce the manufacturing cost as much as possible, bearings were made in a square shape without any bonded thick end plates so that in real practice they can be easily cut to size from a strip FREI. Additionally, being square, identical mechanical properties in the two perpendicular directions of movement can be achieved.

As a novel application, square FREI bearings can be simply placed between the superstructure and foundation with no bonding at the contact surfaces. As a result, the installation of the isolator units is significantly easier and is well suited where no detachment, due to overturning, occurs between the superstructure and isolators. An additional advantage is that the isolator units are placed relatively close together. Therefore, the reinforced concrete beams, which are constructed above the isolators to support the superstructure between isolators, are not required to be heavily reinforced. As a result, no major additional cost is imposed on the construction of the base isolated building.

This paper includes a brief literature review on FREIs, and presents the results of an experimental program conducted on handmade square carbon-FREIs. Stable rollover deformation of bearings as a unique characteristic of using FREIs with unbonded boundary conditions at contact surfaces, is introduced and subsequently discussed.

### **Literature Review**

Kelly (1999) conducted an experimental study on cylindrical handmade bearings consisting of high damped rubber reinforced with Kevlar fibers. From the test results, it was revealed that fiber reinforcement can provide acceptable compression stiffness. Additionally, lack of flexural rigidity of reinforcement was shown to have a small effect on the horizontal stiffness of the bearing. The generated hysteresis loops under combined compression and shear showed the same general characteristics as a traditional SREI bearing with a stable behavior up to a peak shear strain of 150%. Furthermore, damping ratios higher than anticipated were obtained which revealed a new source of energy dissipation. This was an unexpected advantage of using fiber as reinforcement in elastomeric bearings.

Seven rectangular carbon-FREIs were tested (Kelly 2002) under both a compression load (to measure the compression stiffness) and a combination of compression and shear loading (to measure the horizontal stiffness and effective damping). For the latter case, the test was repeated for orientations of 0, 90, and 45 degrees with respect to the longitudinal direction of the strip. It was observed that loading along 0 degree produces stiffening in the hysteresis loops, whereas along 90 degrees (i.e., the cross direction) softening behavior tends to occur. Loading along 45 degree produced neither softening nor stiffening. Experimental results confirmed that it is possible to produce a strip FREI that matches the behavior of a SREI. The measured horizontal stiffnesses and the maximum accommodated displacement indicated that the concept of carbon strip-FREI is viable.

Moon et al. (2003) compared the performance of a cylindrical carbon-FREI to that of the same size SREI. The difference between the steel plate and the fiber thickness was adjusted by using more layers of fiber and rubber in the FREI. Accordingly, bulging of the FREI was smaller than that of the SREI due to the thinner layers of rubber in the FREI. Unlike previous studies (Kelly 1999, and 2002) where the bearings were built without end plates and were not bonded to the test machine during the test, both bearings were

bonded to thick end plates. The researchers concluded that the performance of the FREI is superior to that of the SREI. However, due to insufficient information regarding the details of the tested isolators, the basis of comparison is not clearly identified. Accordingly, comparative studies between FREIs and SREIs still need to be conducted.

Summers et al. (2004) conducted an experimental study on prototype rectangular carbon FREIs as a potential seismic protection strategy for liquid storage tanks. The bearings consisted of high damped rubber compound and were subjected to a maximum 100% shear deformation under constant vertical compression. The resulting hysteresis loops showed stable behavior.

### **Research Objectives**

The main objective of this research project is to evaluate the design properties including displacement characteristics and damping properties of square carbon-FREI bearings through vertical and horizontal cyclic tests. As mentioned previously, the bearings are for application of seismic isolation in ordinary low-rise residential or commercial buildings. To reduce both construction and labor costs, the bearings are simply placed between the superstructure and foundation with no bonding at the contact surfaces. To simulate this novel application, isolator bearings are not bonded to the test machine. The viability of this special application and the effectiveness of employing carbon-FREIs as a seismic isolation device are examined through cyclic test results.

### **Test Specimens**

Two carbon-FREI bearings were built at the Applied Dynamic Laboratory (ADL) of McMaster University. Each bearing consisted of bonded layers of intermediate elastomer and reinforcement as well as two bonded thinner elastomeric covers at the top and bottom. The total thickness of rubber layers was  $t_r = 94$  mm. The width was  $b = 200$  mm and the total height was approximately  $h = 105$  mm. The shape factor (defined as the ratio of loaded area to load free area of the elastomer layer) was  $S = 10.6$  and the aspect ratio (i.e., width to total height ratio, sometimes called second shape factor) of the bearings was approximately  $R = 1.9$ . The elastomer was a soft compound of natural gum rubber with a hardness of 40 Durometer and bi-directional carbon fiber fabric was utilized as the reinforcement. The bearings were made without the use of a mold and all vertical faces were trimmed with a band saw. A finishing coat of bonding compound was applied to the vertical faces of each bearing to prevent any premature delamination.

### **Test Setup and Instrumentation**

Figure 1a shows a sketch of the test setup which is designed to perform both the vertical and horizontal (cyclic) testing on the prototype bearings. The bearing is located between two 100 mm thick steel platens. Horizontal displacements are imposed via a horizontal hydraulic actuator attached to the lower platen. The lower platen is mounted on four linear bearings and can move  $\pm 150$  mm with respect to the upper platen. The upper platen is braced to the body of the horizontal actuator at its lateral sides through two arms providing a self-equilibrating system. The bearing is subjected to near pure shear as the action and the reaction horizontal forces pass through its midheight.

Figures 1b and 1c illustrate the instrumentation used for the test setup. Load cell LC#1 is used to measure the horizontal loads corresponding to different horizontal deflections imposed on the bearing. The relative horizontal movements between the lower and upper platens are monitored through a string pot (SP#1 in Fig. 1a). Four Laser Displacement Transducers (LDT#1 to LDT#4) are used to measure the vertical deflection of the bearing at its four sides during the vertical testing. The vertical deflection is calculated by taking the average value of the LDTs readings. To achieve a symmetrical setup, four identical load cells (i.e., LC#2 to LC#5) are used to measure the vertical load. Steel bearings are placed

between the upper platen and these four load cells to ensure minimum horizontal load will be transferred to the load cells measuring the vertical load.

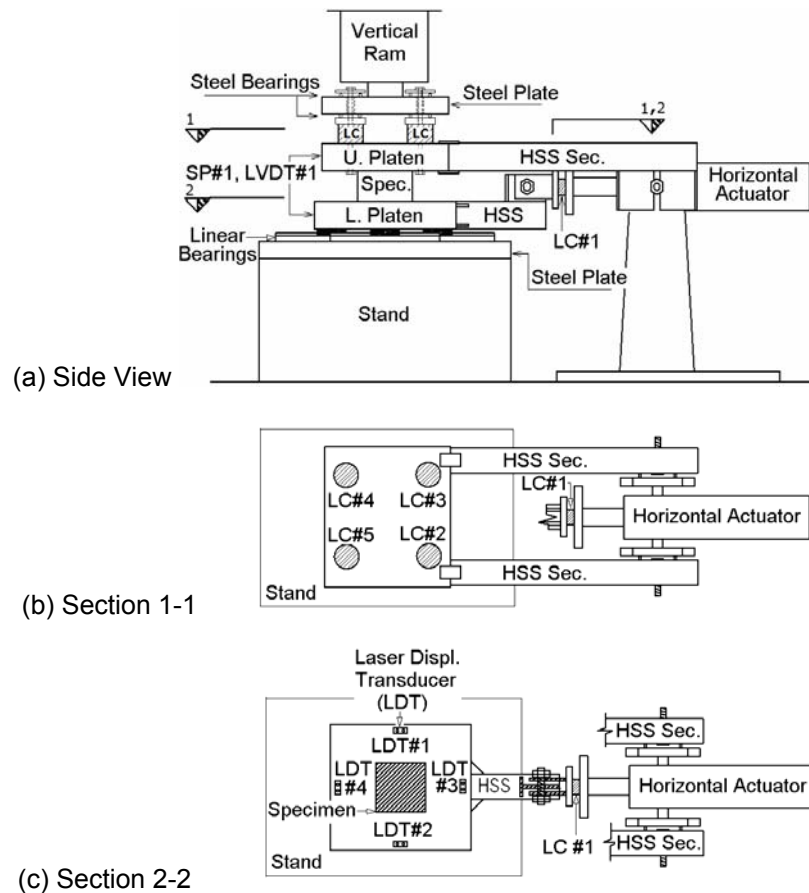


Figure 1. Test setup and instrumentation arrangement.

### Vertical Test

The vertical compression modulus as well as the maximum vertical deflection of the bearings was evaluated through vertical testing, which was conducted in a load control manner. The bearing was monotonically loaded up to 1.6 MPa design vertical pressure (64 kN). Next, three fully reversed cycles with  $\pm 0.35$  MPa variation with respect to the design vertical pressure were performed, and subsequently the bearing was monotonically unloaded. Figures 2a and 2b present the results of the vertical test on Bearings B1 and B2, respectively. The photo in each figure shows the corresponding test in progress. The slope of the dashed straight line represents the average stiffness of each bearing during the cyclic reversals of loading.

From the test results, the vertical stiffness of the bearings were calculated as;  $(K_v)_{B1} = 76.13$  kN/mm, and  $(K_v)_{B2} = 72.87$  kN/mm. These correspond to effective compression modulus values of  $(E_c)_{B1} = 178.9$  MPa,  $(E_c)_{B2} = 171.2$  MPa, and effective vertical frequency values of  $(f_v)_{B1} = 17.2$  Hz, and  $(f_v)_{B2} = 16.8$  Hz, respectively, which are considered satisfactory values for isolation applications (Kelly 2002). Accordingly, these bearings provide sufficient vertical stiffness for vertical pressures around the design value of 1.6 MPa.

As illustrated in Figs. 2a and 2b, both bearings show a significant run-in before developing any vertical stiffness. Results of tensile tests conducted on coupon specimens, made from the carbon reinforcement sheets showed a similar pattern in the tensile load vs. longitudinal deflection. This indicates that carbon fibers in the handmade bearings were not sufficiently taut to prevent initial vertical setting. However, since the required compression modulus is developed at design vertical pressure, this is not considered a significant shortcoming.

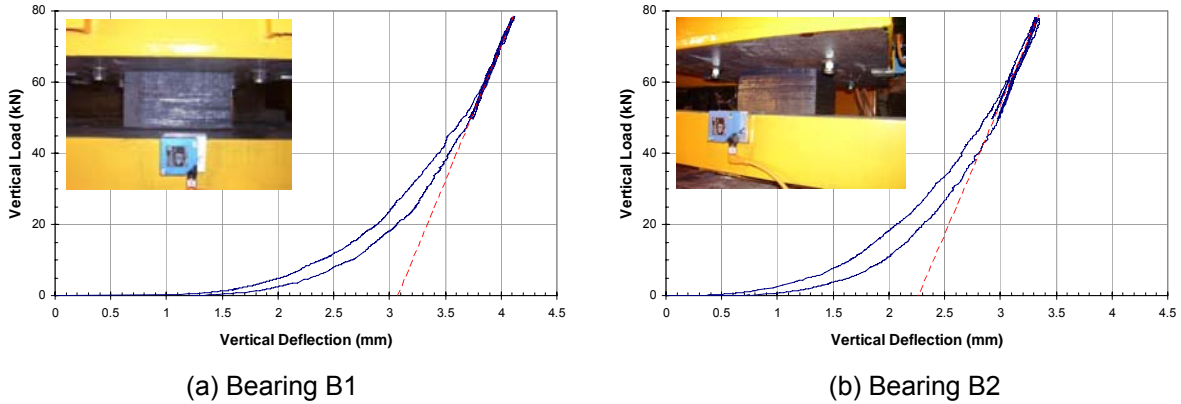


Figure 2. Vertical load – deflection relationship under 64 kN vertical load for Bearings B1 and B2.

### Cyclic Tests

#### Test Procedure and Calculations

Cyclic tests on prototype isolators provide one of the most reliable methods to identify the deformation characteristics and damping values of any isolation system. Cyclic tests are performed under horizontal displacement control and vertical load control. The test procedure used in this research study was as follows: while the bearing was subjected to a constant vertical pressure, four fully reversed sinusoidal cycles of horizontal displacements having amplitudes of 25%  $t_r$ , 50%  $t_r$ , 75%  $t_r$ , 100%  $t_r$ , 125%  $t_r$ , 150%  $t_r$ , and 200%  $t_r$  (where  $t_r$  is the total thickness of rubber layers in each bearing) were applied. For each amplitude, the bearing was vertically loaded up to the target load. Subsequently, four cycles of horizontal displacement were applied after which the bearing was vertically unloaded.

As a simple calculation, the bearing's effective horizontal stiffness, corresponding to each load cycle of the test, can be calculated based on the peak lateral load and peak displacement as follows (ASCE 7, 2005);

$$K_{h,eff} = (F_{max} - F_{min}) / (\Delta_{max} - \Delta_{min}) \quad (1)$$

Where  $F_{max}$ ,  $F_{min}$ ,  $\Delta_{max}$  and  $\Delta_{min}$  are the maximum and minimum values of horizontal load and horizontal displacement, respectively. The ratio of equivalent viscous damping of the bearing at each cycle is given below (Clough and Penzien 1975);

$$\xi = W_d / (4\pi W_s) \quad (2)$$

Where  $W_d$  and  $W_s$  represent the dissipated energy (area within the hysteresis loop) and the restored (elastic) energy, respectively. Having  $\Delta_{ave,max} = (\Delta_{max} + |\Delta_{min}|) / 2$ , the following formula defines  $W_s$  as

$$W_s = \frac{1}{2} K_{h,eff} \Delta_{ave,max}^2 \quad (3)$$

### Cyclic Test on B1 and B2

The horizontal load-displacement behavior of Bearings B1 and B2 at different values of peak horizontal displacement was found to be similar. Accordingly, only experimental results of Bearing B1 are presented in this paper. Figure 3a shows the horizontal load-displacement curves of Bearing B1 subjected to 25, 50, 100, and 125%  $t_r$  horizontal displacement. As illustrated, the bearing behaves linearly up to approximately 75%  $t_r$  horizontal displacement with an effective horizontal stiffness  $K_{h,B1} = 0.13$  kN/mm and 2.1% effective damping ratio calculated using equations (1) & (2), respectively. At larger lateral displacements, nonlinear response with a tendency of softening can be observed. This softening is associated with the rollover deformation of the bearing which resulted from the boundary conditions at its contact surfaces.

To study the influence of higher vertical pressure on improving the horizontal response of the bearing, cyclic tests were duplicated under a larger constant vertical pressure of 3.2 MPa (see Fig. 3b). At 75%  $t_r$  horizontal displacement, the effective horizontal stiffness of the bearing decreased to 0.12 kN/mm and the effective damping ratio increased to 5.2%. A significant increase in the damping ratios of FREIs due to higher vertical pressure is a unique feature not found in SREIs. This fact reveals one of the advantages of using fibers as the reinforcement (Kelly 1999). At lateral displacements larger than 75%  $t_r$ , as indicated in Fig. 3b the bearing performs nonlinearly and again tends to show a softening type behavior even though a higher vertical pressure (twice as large as the design value) was applied.

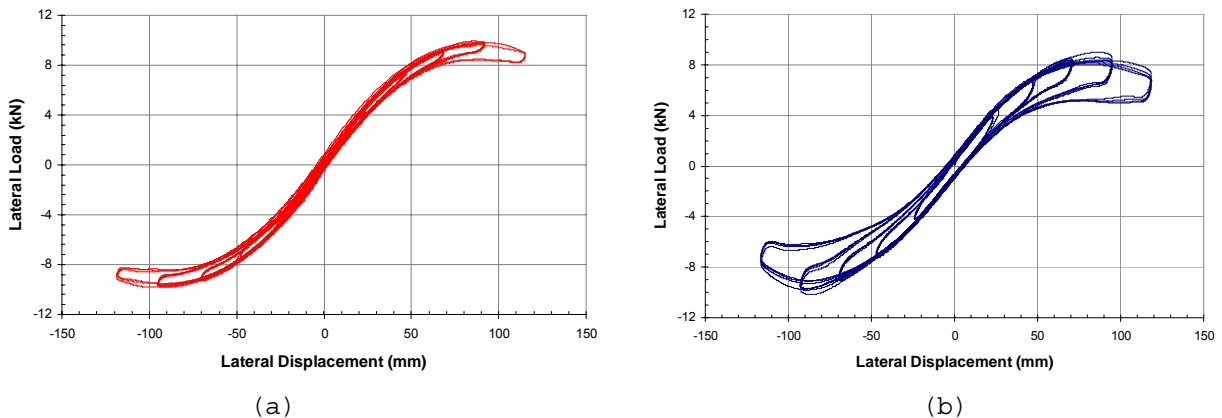


Figure 3. Lateral load-displacement behavior for Bearing B1 (aspect ratio  $R_{B1} = 1.9$ , and  $t_{r,B1} = 94$  mm), in a series of cyclic tests having amplitudes of 25, 50, 75, 100, and 125%  $t_{r,B1}$ , under constant vertical compression (a) 1.6 MPa, (b) 3.2 MPa.

No damage was visible after the cyclic tests were completed. Furthermore, the repeatable pattern of the load hysteresis loops, including the maximum lateral displacements, implied that negligible damage occurred to the bearings. As a result of the softening behavior, the performance of Bearings B1 and B2 with an aspect ratio of  $R = 1.9$  was considered unacceptable. In an attempt to improve the lateral load-displacement behavior of the bearings, the aspect ratio was increased by reducing the bearing thickness. In order to study the influence of different aspect ratios on improving the lateral response of the bearings, new Bearings NB1 and NB2 were cut from B1 and B2 to achieve aspect ratios of  $R_{NB1} = 2.5$  and  $R_{NB2} = 2.9$ , respectively.

### Cyclic Test on NB1

Figure 4a shows the hysteresis loops of NB1 when subjected to cyclic lateral displacements with different amplitudes ranging from 25% to 200%  $t_{r,NB1}$  (where total thickness of rubber layers  $t_{r,NB1} = 70.5$  mm).

As illustrated in Fig. 4a, the bearing performs almost linearly to 75%  $t_r$ ,  $t_{r, NB1} \approx 53$  mm lateral displacement with an effective stiffness  $K_{h, NB1} = 0.21$  kN/mm and effective damping ratio of 1.5%. However, at larger lateral displacements, due to the rollover deformation of the bearing, the tangent horizontal stiffness dramatically drops to its minimum-yet-positive value. At extreme lateral displacements (larger than 150%  $t_r$ ,  $t_{r, NB1}$ ) when the vertical faces of the bearing contact the upper and lower platens (see Fig. 5c), a hardening behavior is observed. This is considered to be advantageous as it imposes a limit on the maximum lateral displacement of the bearing and guarantees stability of the device against the maximum considered earthquake. Figure 5 shows photographs taken from cyclic testing on Bearing NB1 at different extreme lateral displacements.

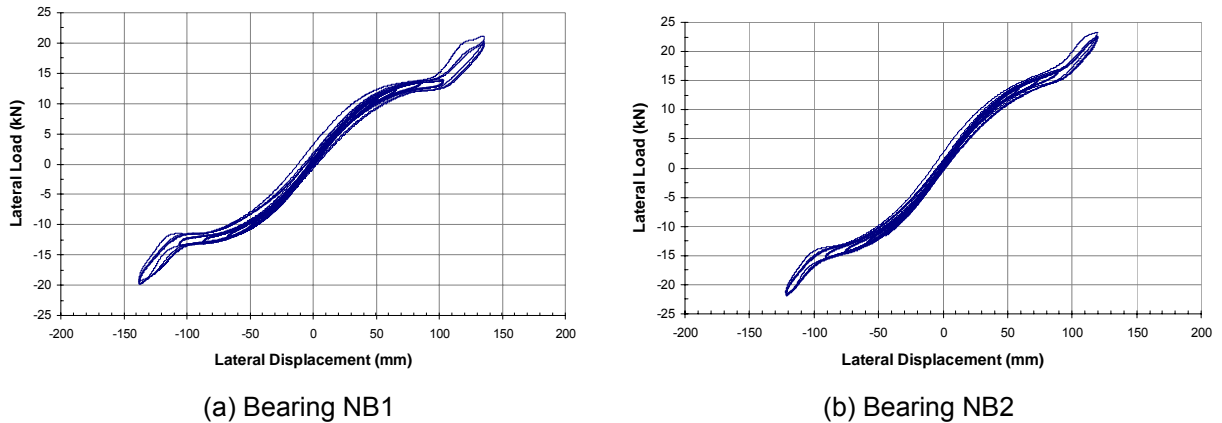


Figure 4. Lateral load displacement behavior, under constant 1.6 MPa vertical compression, in a series of cyclic tests having amplitudes 25, 50, 75, 100, 125, 150, and 200%  $t_r$  for (a) Bearing NB1 (aspect ratio  $R_{NB1} = 2.5$ , and  $t_{r, NB1} = 70.5$  mm), and (b) Bearing NB2 (aspect ratio  $R_{NB2} = 2.9$ ,  $t_{r, NB2} = 61.1$  mm).

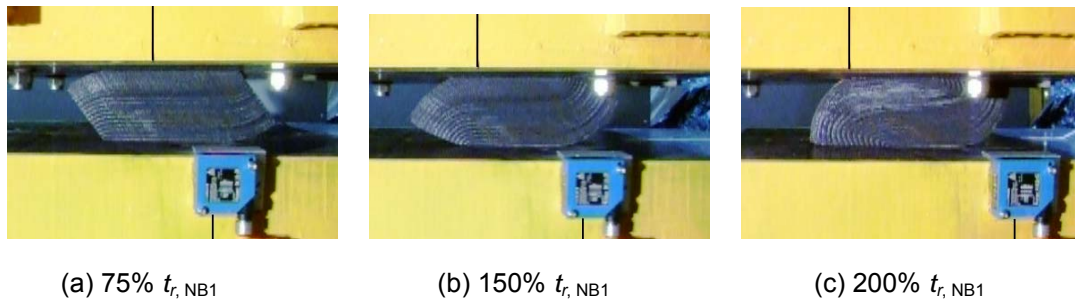


Figure 5. Bearing NB1 ( $t_{r, NB1} = 70.5$  mm) under constant vertical 1.6 MPa compression, subjected to different lateral displacements.

### Cyclic Test on NB2

Bearing NB2, with a total thickness of 69 mm, was cut through the thickness of Bearing B2 so that an aspect ratio of  $R_{NB2} = 2.9$  was achieved. As a result, the total thickness of rubber layers of the bearing was reduced to  $t_{r, NB2} = 61.1$  mm.

Figure 4b shows the hysteresis loops from a set of cyclic tests conducted on Bearing NB2. This bearing showed a linear behavior up to approximately 75%  $t_r$ ,  $t_{r, NB2} \approx 46$  mm lateral displacement with an effective stiffness  $K_{h, NB2} = 0.25$  kN/mm and an effective damping ratio of 1.3%. However, due to rollover deformation at larger lateral displacements, the tangent horizontal stiffness of the bearing gradually

decreased to its minimum value. Analogous to Bearing NB1, at extreme lateral displacements when the vertical faces of bearing contacted the upper and lower platens, a hardening behavior was observed.

## Discussion of Cyclic Test Results

### Performance Observations

In this study, all bearings exhibited a rollover deformation when subjected to lateral loads. This rollover deformation results from the unbonded boundary condition of the bearing at its contact surfaces as well as the lack of flexural rigidity in the fiber reinforcement layers. This deformation, which causes a significant reduction in the horizontal stiffness of the bearing, is considered acceptable if the resulting tangent horizontal stiffness of the bearing remains positive. In such a case, when the vertical faces of the bearing touch the upper and lower platens at the extreme lateral displacements, a hardening behavior is observed. This hardening places a limit on the maximum lateral displacement of the bearing and ensures its overall stability. We denote such an admissible deformation hereafter as a stable rollover deformation. A stable rollover deformation neither results in a softening behavior nor does it compromise the overall stability of the bearing. Furthermore, being a seismic isolation device, it adds to the efficiency of the bearing as the horizontal stiffness is reduced. As a result, this unique performance is considered advantageous for application of FREIs with unbonded contact surfaces.

Considering all the bearings tested in this research project, the lateral load-displacement performance of Bearings B1 and B2 is not acceptable as they exhibited softening and negative tangent horizontal stiffness due to unstable rollover deformation (Fig. 3a). The same unacceptable behavior was observed when the vertical compression was doubled (Fig. 3b). It was found that, for a FREI with the same material properties and shape factor ( $S$ ), the aspect ratio ( $R$ ) of the bearing plays a crucial role in achieving a stable rollover deformation.

Similar to SREI behavior, an increase in the vertical pressure reduces the horizontal stiffness of a FREI. However, a higher vertical pressure results in an increase in the energy dissipated by a FREI (see Figs. 3a and 3b). This is attributable to an increase in the in-plane tension in the fibers. Carbon fiber fabric consists of strands of fibers woven together. When a FREI bearing is deformed laterally, the reinforcement layers are curved due to lack of flexural rigidity. Accordingly, the in-plane tension in the curved fibers forces the strands to slip against each other dissipating energy through friction (Kelly 1999).

### Discussion on Results of Bearing NB1

As illustrated in Fig. 4a, the nonlinear behavior of Bearing NB1, due to a stable rollover deformation, has three distinct response components and can be modeled with a simple trilinear idealized model. For minor earthquakes, the bearing can be designed to remain within its initial stage of lateral load-displacement response with an effective horizontal stiffness  $K_{h1, NB1} = 0.21$  kN/mm. To achieve the maximum efficiency against Design Basis Earthquakes (DBE with approximately 10% probability of exceedance within 50 years), the effective horizontal stiffness drops to the minimum value  $K_{h2, NB1} = 0.13$  kN/mm. At Maximum Considered Earthquake (MCE), with 2% probability of exceedance within 50 years (2,500 year return period), the bearing is allowed to undergo larger lateral displacements and exhibits a hardening behavior. The effective horizontal stiffness at the latter case will be  $K_{h3, NB1} = 0.15$  kN/mm.

An initial horizontal stiffness of 0.21 kN/mm, in a bearing subjected to a constant vertical compression of 1.6 MPa, results in an isolated period of 1.1 s. However, depending on the magnitude of earthquake energy, the effective horizontal stiffness can drop to as low as 0.13 kN/mm and the isolated period can reach a value of 1.4 s which results in increased seismic mitigation.

At DBE, the design lateral displacement of Bearing NB1, can vary between 100% to 150%  $t_{r, NB1}$  (70 mm to 105 mm). Test results have shown that NB1 can sustain large cyclic lateral displacements up to a

maximum value 140 mm (200%  $t_{r,NB1}$ ) with no significant stiffness degradation. Furthermore, after the completion of the cyclic tests no delamination or any other damage was observed in the bearing. Accordingly, at MCE, an upper limit of 140 mm can be accepted for design purposes as the maximum admissible lateral displacement of this bearing.

Due to the smaller total volume of carbon fiber reinforcement utilized in NB1, this bearing exhibited lower damping ratios than Bearing B1. Depending on the amplitude of lateral displacement, effective damping of Bearings NB1 varies from 1% to 3% which is less than the required value.

### **Discussion on Results of Bearing NB2**

Comparing Figs. 4b and 4a, the nonlinear behavior of Bearing NB2 is not as significant as NB1, nevertheless, it can be modeled with a simple trilinear idealization. The effective horizontal stiffnesses of NB2 corresponding to 75, 125, 150, and 200%  $t_{r,NB2}$  lateral displacements were calculated to be 0.25, 0.20, 0.18, and 0.18 kN/mm, respectively. Therefore, the isolated period of Bearing NB2 will fluctuate between 1 s to 1.2 s. In contrast to NB1, the effective horizontal stiffness of NB2 gradually decreases with an increase in the amplitude of lateral displacement.

The smaller volume of carbon fiber reinforcement on NB2, compare to that of NB1, implies lower damping ratios of Bearing NB2. Test results confirmed this expectation. Depending on the amplitude of lateral displacement, the effective damping of Bearing NB2 varied from 0.8% to 2.3%.

After completion of the cyclic tests, no damage in NB2 was visible. Additionally, the stable pattern and repeatability of hysteresis loops at different displacement amplitudes, including 122 mm (200%  $t_{r,NB2}$ ), indicated that no noticeable damage had occurred inside the bearing. As a result, the bearing can be safely subjected to the maximum 122 mm lateral displacement.

The efficiency index of a bearing with nonlinear lateral load-displacement behavior can be defined as the ratio of maximum instant isolated period to the minimum achievable isolated period. This ratio for Bearings NB1 and NB2 are 1.27 and 1.20, respectively. Therefore, NB1 provides more seismic mitigation than NB2. As a result, for a FREI bearing with the given width, shape factor, vertical load, and elastomer modulus, by providing higher efficiency, an aspect ratio of 2.5 is close to the optimum value for the application considered in this study.

### **Conclusions**

Results of an experimental study conducted on handmade square carbon-FREI bearings employing soft compound low damped natural rubber as the elastomer are presented in this paper. The bearings are meant to be used for base isolation of ordinary low-rise residential and commercial buildings. As a special application, the bearings were not bonded to the test platens. For bearings having suitable aspect ratio values (i.e., NB1 and NB2), this particular type of application has resulted in a stable rollover deformation, which reduced the horizontal stiffness and increased the efficiency of the bearing as a seismic isolation device.

Cyclic tests on Bearings NB1 and NB2 showed that the isolated period of these bearings, depending on the severity of earthquake, will vary between 1.1 to 1.4 s and 1.0 to 1.2 s, respectively. Furthermore, NB1 and NB2 were tested at up to 140 mm and 120 mm lateral displacement, respectively. These values are considered to be sufficient (ASCE 7, 2005) for many high seismic risk regions in Canada including Vancouver and Victoria, provided that at least 5% effective damping can be achieved in the isolation system. Test results suggest that application of these bearings can significantly reduce the earthquake induced force and interstory drift in a masonry shear wall structure with a fixed-base period in the range of 0.1 s.

Vertical testing revealed that carbon fiber reinforcement provides an acceptable vertical stiffness in FREI bearings. A vertical frequency of around 17 Hz was achieved in Bearings B1 and B2, which is considered as an acceptable value for seismic isolation application. Due to the shorter height, Bearings NB1 and NB2 exhibit even larger vertical stiffnesses compared to Bearings B1 and B2.

A low damping ratio and lack of sufficient horizontal stiffness against service lateral loads are two shortcomings of the bearings tested in this research program. No information was provided by the supplier of the natural rubber about the effective damping of the elastomer used in the bearings. However, low damping ratios of all bearings indicated the inherent damping in soft compounds of natural rubber is so low that even the additional source of energy dissipation due to the use of fiber reinforcement cannot provide the required amount of damping for a seismic isolation device subjected to relatively light vertical pressure. The low initial horizontal stiffness of the bearing implies that lateral displacements due to service lateral loads such as wind loads may exceed the admissible limits. These issues can be easily resolved by utilizing a high damped rubber with high initial shear modulus and higher damping properties, or using supplementary devices to provide higher initial stiffness and higher damping ratios.

### Acknowledgments

This research was carried out as part of the mandate of the McMaster University Centre for Effective Design of Structures funded through the Ontario Research and Development Challenge Fund. The authors also would like to gratefully acknowledge the Ministry of Science, Research and Technology of Iran and the Natural Sciences and Engineering Research Council of Canada (NSERC).

### References

- ASCE 7, American Society of Civil Engineers, 2005. *Minimum Design Loads for Buildings and Other Structures*, ASCE/SEI 7-05.
- Clough, R., and Penzien, J., 1975. *Dynamics of Structures*, McGraw-Hill, New York.
- Kang, B. S., Kang, G. J., Moon, B. Y., 2003. Hole and Lead Plug Effect on Fiber Reinforced Elastomeric Isolator for Seismic Isolation, *Journal of Material Processing Technology*, 140, 592-597.
- Kelly, J. M., 1999. Analysis of Fiber-Reinforced Elastomeric Isolators, *Journal of Seismology and Earthquake Engineering (JSEE)*, 2 (1), 19-34.
- Kelly, J. M. 2002. Seismic Isolation Systems for Developing Countries, *Earthquake Spectra*, 18 (3), 385-406.
- Moon, B. Y., Kang, G. J., Kang, B. S., Kelly, J. M., 2002. Design and manufacturing of fiber reinforced elastomeric isolator for seismic isolation, *Journal of Materials Processing Technology*, 130–131, 145–150.
- Moon, B. Y., Kang, B. S., and Kim, H. S., 2003. Mechanical Property Analysis and Design of Shock Absorber System Using Fiber Bearing by Experimental Method, *JSME International Journal*, 46 (1), 289-296.
- Naeim, F., and Kelly, J. M., 1999. *Design of Seismic Isolated Structures*, John Wiley, New York.
- Summers, P., Jacob, P., Marti, J., Bergamo, G., Dorfmann, L., Castellano, G., Poggianti, A., Karabalis, D., Silbe, H., and Triantafillou, S., 2004. Development of new base isolation devices for application at refineries and petrochemical facilities, *13<sup>th</sup> World Conference on Earthquake Engineering Vancouver, B.C., Canada, August 1-6*, Paper No. 1036.